

Unsupervised Neural Network for Tool Breakage Detection in Turning

V. B. Jammu, K. Danai/S. Malkin (1), University of Massachusetts, Amherst/USA

Received on January 13, 1993

An unsupervised neural network is introduced for on-line tool breakage detection in machining using multiple sensors. This neural network performs detection by classifying the measurements either as normal or abnormal. However, it performs classification by relying only on the normal category, so that it does not need to establish the abnormal category requiring samples of measurements taken at tool breakage. This *Single Category-Based Classifier (SCBC)* also adapts the prototype values on-line so as to continuously update the normal category, and employs the noise suppression techniques: *contrast enhancement* and *voting*, in order to cope with different levels of noise in measurements. The performance of the SCBC is evaluated in turning. Extensive tests were performed which produced six tool breakage cases. Four measurements which were clear indicators of tool breakage in these tests were used as inputs to the SCBC and to two other classifiers utilizing Kohonen's Feature Mapping and Adaptive Resonance Theory (ART2). The results indicate that the SCBC was the only classifier that could detect all of the tool breakages.

1 INTRODUCTION

On-line detection of tool breakage in machining is important for automation. The traditional approach to tool breakage detection has focused on the development of signal processing techniques that can enhance the effect of tool breakage (tool breakage signature) on measurements of the cutting force [6], acoustic emission [11,8], spindle motor current [10], etc. The effect of tool breakage is usually revealed from an abrupt change in these processed measurements, in excess of a threshold value. Although these techniques are generally effective for specific cutting conditions, they are often not sufficiently reliable for use in production due to the inability of single measurements to reflect the effect of tool breakage under diverse cutting conditions.

In order to enhance the reliability of tool breakage signatures obtained from single sensors, an integrated approach based on measurements from several sensors has been proposed [2]. With the multi-sensor approach, the tool breakage signature becomes multi-dimensional and needs to be identified through pattern classification. Artificial neural networks are often used for pattern classification with connection weights representing decision regions for various categories. Ideally a neural network is trained to identify the tool breakage signature by supervised learning, which necessitates providing samples of measurements taken at tool breakage. However, sufficient tool breakage data may not be available, thereby limiting the effectiveness of supervised neural networks for this purpose.

It is proposed that unsupervised neural networks be used for on-line tool breakage detection in machining [12]. The two predominant methods of unsupervised learning presently available for neural networks are Kohonen's Feature Mapping [7] and Adaptive Resonance Theory (ART2) [1,4]. Kohonen's method of feature mapping establishes the decision regions for normal and abnormal categories through prototype vectors which represent the centers of measurement 'clusters' belonging to these categories. Classification is based on the Euclidean distance between the measurements and each of the prototype vectors. While the Kohonen's method forms the prototype vectors far enough from each other to cope with variations in the tool breakage signature, it requires one or more sets of measurements at tool breakage in order to establish the prototype vector for the abnormal category. The other method of unsupervised learning, the Adaptive Resonance Theory (ART2), classifies the measurements as normal unless they are 'sufficiently different'. When applied to tool breakage detection [12] it does not require any samples of measurements taken at tool breakage. However, the ART2 method cannot effectively cope with varying levels of noise associated with different sensors. Moreover, classification in ART2 depends upon a *vigilance function* to characterize the similarity between measurements and prototypes of various categories. Since the *vigilance function* has the property of categorizing multiples of a prototype within the same category, it has a high tendency for misclassification.

In this paper a new unsupervised method of learning for neural networks is introduced that is ideally suited to tool breakage detection using multiple sensors. This method is designed such that it only needs to define the prototype vector for the normal category and, as such, can be referred to as a *Single Category-Based Classifier (SCBC)*. It performs detection by comparing each set of measurements against corresponding prototype values for their normal category. Tool breakage is assumed to have occurred when the measurements are "sufficiently different" from their normal prototypes. The difference between the measurements and their normal prototypes in the SCBC is determined by a *matching factor* based on the Euclidean distance of the measurements from the prototype values. Noise suppression techniques are used to cope with different noise levels in individual measurements.

2 SINGLE CATEGORY-BASED CLASSIFIER (SCBC)

Detection in the SCBC is performed by classifying the measurement vector $S(t) = [s_1(t), s_2(t), s_3(t), \dots, s_n(t)]$ as normal or abnormal. In this classifier,

only the normal category is defined by a prototype vector $W = [w_1, w_2, \dots, w_n]$, and classification is performed by measuring the similarity of each measurement s_i to its corresponding prototype value w_i based on a *matching factor* ϕ_i , defined as

$$\phi_i = \frac{[s_i(t) - w_i]^2}{w_i^2} \quad (1)$$

The measurements $s_i(t)$ are classified as normal if the ϕ_i values are less than or equal to a threshold quantity h :

$$\begin{cases} \phi_i \leq h & \text{then } f_i(t) = 0 \\ \text{otherwise} & f_i(t) = 1 \end{cases} \quad (2)$$

The f_i are binary representations of s_i and the threshold h is specified as:

$$h = \frac{1}{n} \sum_{i=1}^n \frac{[\max(s_i) - \mu_i]^2}{\mu_i^2} \quad (3)$$

where $\max(s_i)$ is the maximum value of the i th measurement in a set of k samples of this measurement recorded during normal operation, and μ_i is the mean value of the i th measurement in this sample set estimated as

$$\mu_i = \frac{1}{k} \sum_{t=1}^k s_i(t) \quad (4)$$

After all the measurements are classified, they are represented by a binary vector $F(t) = [f_1(t), f_2(t), \dots, f_n(t)]$, and then integrated through voting. The process is classified as normal when

$$\frac{1}{n} \sum_{i=1}^n f_i \leq 0.5 \quad (5)$$

or otherwise as abnormal.

After classification of each measurement vector, the prototype values in the SCBC are updated so as to adapt to changing process conditions and measurement noise. Adaptation is performed as follows: let w_I represent the prototype value which is presently being updated and w_i represent the remaining prototype values. The adaptation algorithm first modifies the prototype value w_I according to the relationship

$$w_I = w_I + \delta w_I \quad (6)$$

where

$$\delta w_I = \begin{cases} \eta [s_I(t) - w_I] & \text{if } f_I(t) = 0 \\ 0 & \text{otherwise} \end{cases} \quad (7)$$

The parameter η in Eq. (7) denotes the learning rate.

The SCBC also incorporates noise suppression by *contrast enhancement* [1], whereby prototype values are adapted so as to increase homogeneity of classification among measurements. Based on this feature, if the majority of measurements are classified as normal, then prototype values associated with the measurements classified as abnormal are adjusted such that the likelihood of all the measurements classified as normal is increased for the same measurement values. *Contrast enhancement* has the form

$$w_i = w_i + \delta w_i \quad \text{for all } i \neq I \quad (8)$$

where

$$\delta w_i = \begin{cases} \eta \Lambda [s_i(t) - w_i] & \text{if } f_I(t) = 0 \\ 0 & \text{otherwise} \end{cases} \quad (9)$$

In the above adaptation scheme, the amount by which the prototype values are adjusted is controlled by a *neighborhood function* Λ [7] which is assigned a value between 0 and 1. A value of 0 is used for inputs with no noise, whereas a value at the other extreme of 1 is for unreliable measurements with large amounts of noise. In practice, the value of Λ does not exceed 0.5.

In the training algorithm (Eqs. (6) and (7)), I is varied from 1 to n in order to adapt all the prototype values w_I . For each I the remaining prototype values w_I are adapted according to Eqs. (8) and (9).

The adaptation algorithm presented in Eqs. (6)-(9) is biased towards the most recent measurement vector. Ideally, adaptation should be performed using all the measurement vectors, but as the number of available measurement vectors progressively increases training on all the measurements becomes computationally exhaustive. As a compromise, only the present and m most recent measurement vectors are utilized for each adaptation sweep in the SCBC, such that adaptation is performed iteratively over the $m + 1$ most recent measurement vectors, with the learning rate η progressively decreasing for each training iteration.

The SCBC is implemented using the neural network illustrated in Fig. 1. Inputs to this network are the measurements, which are often pre-processed through the 'Signal Processing' block to enhance the effect of tool breakage. Its outputs are binary numbers, 0 denoting classification as normal and 1 as abnormal. Weights between inputs and outputs in this network denote the prototype values representing the normal category. In the SCBC, the first set of inputs (measurement vector) supplied to the network is assumed to represent the normal category and is used to assign the initial weights. For each subsequent measurement set, the matching factors ϕ_i between each measurement and its prototype is calculated based on Eq. (1) and hard-limited to classify the measurements. The binary measurements are then passed through the 'Voting' block where the process is classified as normal if the majority of measurements have a value of 0.

3 EXPERIMENTAL

The feasibility of the SCBC was evaluated using data obtained from turning experiments on a 37 kW NC vertical turret lathe (LVM125) [2]. The tools used were 35 degree diamond shaped tungsten carbide cam lock inserts and the tool holder used was a MVJNR 24-4 (side cutting edge angle = -3° , side rake angle = $-4^\circ 15'$, back rake angle = $-13^\circ 20'$). Two accelerometers (PCB 308B) were located on the ram of the lathe to measure the vibration in both the X and Y directions as illustrated in Fig. 2. Also located on the ram was a high frequency accelerometer (VM 1000) to measure the ultrasonic energy (UE) of the cutting process in the 20kHz to 80kHz frequency range. Current inputs to the X-carriage and Z-carriage drive motors were measured using a simple shunt resistor. Signals proportional to the velocity components of the feed carriage in both the X and Z directions were obtained from the numerical control unit (GE MC 2000), and the spindle speed was measured by a once per revolution magnetic pickup. All sensory signals were

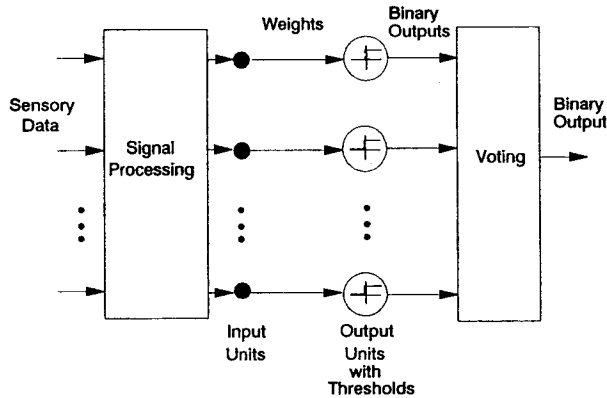


Figure 1: Architecture of the single layer neural network implementing the SCBC.

recorded on a 14 track instrumentation tape recorder, and video images of the cutting tool and numerical control screen, were also recorded together with a special time code signal to synchronize the video record with sensory signals.

Straight internal cuts were taken on Inconel 718 cylindrical workpieces of approximately 48 cm inside diameter with the conditions listed in Table 1. Extensive testing was performed, of which six tests ending with tool breakages were analyzed. All breakage cases resulted in the loss of more than a third of the insert, usually in the middle of the lock pin area. In Tests #1, #2, #4, and #5 the cutting variables were constant, whereas in Tests #3 and #6 the depth of cut was gradually increased until tool breakage occurred.

4 SIGNAL PROCESSING

In order to study the effect of tool breakage on the measurements, the exact time of each tool breakage was determined through video tapes. Thirty second windows centered around these times were then established for digitization purposes. Measurements in these time windows were low-pass filtered at 666 Hz and digitized at a sampling frequency of 2000 Hz. A preliminary

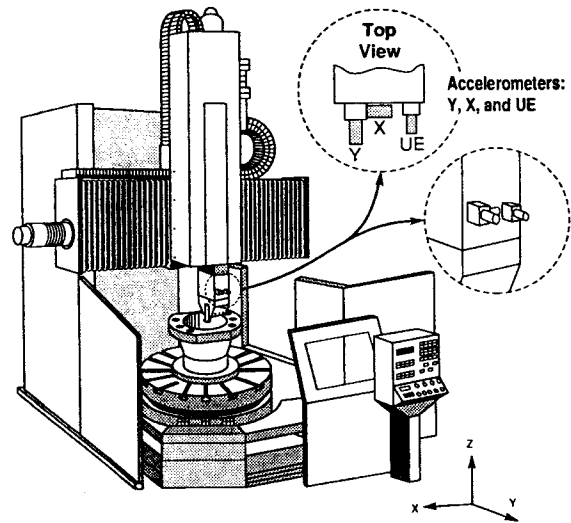


Figure 2: Location of various sensors on the machine tool.

examination of the digitized signals revealed a lag of as much as 0.0105 seconds in the effect of tool breakage on motor currents, which was associated with the response of the machine controller to the change in cutting load caused by tool breakage. In order to resolve this lag differential, so as to have the effect of tool breakage simultaneously reflected by all measurements, the data points contained within each 0.0125 second time interval (25 data points) were block averaged. As a result of block averaging, the data set was reduced to a more manageable size, in effect reducing the sampling frequency to 40 Hz and aliasing the signal. Aliasing was not of major concern here because a frequency domain analysis was not used. In the following, the signal processing applied to each sensory data is discussed separately.

4.1 Ultrasonic Energy

The ultrasonic energy (UE) signal shares the same emission sources as acoustic emission (i.e., deformation in the shear zone, deformation and sliding friction at the tool-chip interface and tool-workpiece interface, and the breaking

Test #	Depth of Cut (mm)	Feed (mm/rev)	Cutting Speed (m/sec)
1	2.03	0.18	0.61
2	2.03	0.18	0.61
3	2.54	0.18	0.61
4	2.03	0.20	0.90
5	2.03	0.20	0.88
6	3.81	0.20	0.88

Table 1: Parameters used in the experiments.

of chips and their impact on the cutting tool or workpiece), but covers a lower frequency range which allows placement of the transducer further away from the cutting zone [3]. The UE signal was measured by an accelerometer operating over a wide band (5Hz to 80kHz). This signal was then amplified, band pass filtered between 20kHz and 80kHz, full wave rectified, and RC averaged (the envelope of this processed signal was extracted) to enhance the effect of tool breakage [3]. Figure 3 shows the processed UE signal in the 30 second time windows for the six tests. The processed UE signal reflects tool breakages (indicated by the asterisks), but also contains other spikes that can be mistaken for tool breakage effects. If used by itself for tool breakage detection the processed UE signal would produce many 'false alarms' depending on the threshold level. If the threshold level is set higher the number of false alarms is reduced but tool breakages may be missed (e.g., in Test #6).

4.2 Low Frequency Vibration

Lower frequency vibrations (below 500 Hz) should be sensitive to loading changes of the tool carriage caused by tool breakage. The vibration signals originally measured in the frequency range of 0 to 666 Hz in the X and Y directions (see Fig. 2) on the ram of the feed carriage are shown in Figs. 4 and 5, respectively, for the selected time windows of the six tests. Both of these signals detect tool breakages (indicated by the asterisks) except in Test # 6, so tool breakage detection based on either of these signals alone would result in at least one 'undetected fault'.

4.3 X and Z Feed Motor Currents and Velocities

A common method of examining abnormalities in a signal is through modeling the signal during normal conditions, so that any mismatch between

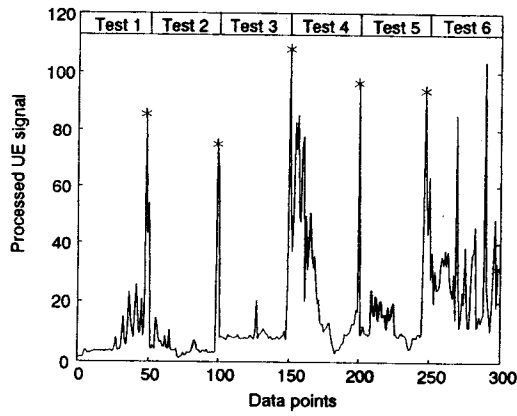


Figure 3: Selected processed UE data for the six tests. Tool breakages are indicated by the asterisks.

the signal and its modelled value can be detected through its residual [5]. Since tool breakage is expected to affect the load of the drive system, an ARX model [9] of the drive system in the Z direction was developed with the Z-current as the input and Z-velocity as the output. One drawback with this model is that it would only represent the dynamics of the feed drive system under nominal friction and cutting loads. Therefore, any cutting load changes due to different cutting variables, hard spots, chip entanglement, or changes in the frictional behavior of the machine ways will be reflected in the residual as noise. While such noise may be significant for machining parts with complex geometry, or interrupted cuts, the cutting load changes in the present experiments were insignificant since the cutting variables were essentially maintained constant in the six tests. Also frictional changes were expected to be small since the machine ways utilized recirculating roller pack bearings.

For modeling purposes, the data from Test #3 were used to develop a fourth order ARX model with one delay based on a 95% confidence interval for both the autocorrelation of the residuals and the cross-correlation between the residuals and the inputs [9]. Figure 6 shows the sensitivity of the residuals obtained by subtracting the output of the ARX model from the

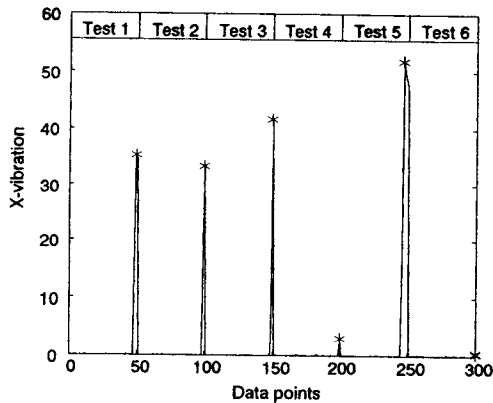


Figure 4: Selected low frequency vibrations in the X direction for the six tests. Tool breakages are indicated by the asterisks.

actual Z-velocity for the time windows of the six tests. The residuals detect tool breakages (indicated by the asterisks) but, like the processed UE signal (Fig. 3), contain many spikes that cannot be distinguished from the effect of tool breakage.

5 DETECTION RESULTS

The effectiveness of the SCBC in tool breakage detection was investigated for this data. Inputs to the SCBC were the four processed measurements obtained from the experiments: (1) processed UE signal, (2) X-vibration, (3) Y-vibration, and (4) residuals of the ARX model between the Z-current and Z-velocity. Each of the data sets from individual tests contained 50 measurement vectors, with each vector consisting of four components as indicated above. At the beginning of each run, initial network weights were established based on the first measurement vector, which was assumed to reflect normal cutting. Measurement sets were then classified as normal or abnormal, with the weights adapted after each classification. The value of the learning rate η was set equal to the inverse of the training iteration in each adaptation sweep over the $m + 1$ most recent measurements. In this

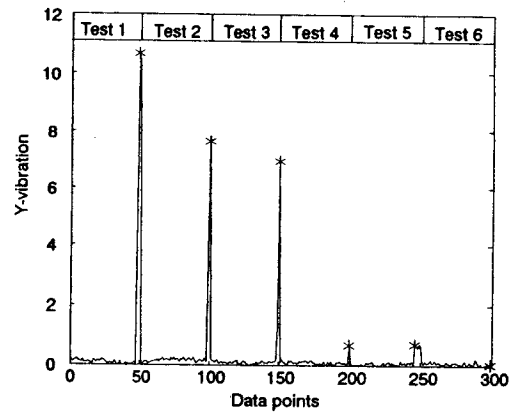


Figure 5: Selected low frequency vibrations in the Y direction for the six tests. Tool breakages are indicated by the asterisks.

application, m was set equal to 30, the neighborhood function Λ was equal to 0.3, and the threshold was established from the normal data in Test #1 at 2.25.

The relative effectiveness of the SCBC was evaluated by comparison with Kohonen's method and ART2. Kohonen's method is a batch type of classifier which requires all of the test sets for training. As such, this classifier is not suitable for on-line detection. The *neighborhood function* for the Kohonen's algorithm was set equal to 0.3. The parameters used for the ART2 algorithm were: the *vigilance function* = 0.9, $a = 10$, $b = 10$, $c = 0.01$, $d = 0.99$, $e = 0.001$, and $\theta = 0.1$.

The detection results obtained from the SCBC, Kohonen's, and ART2 classifiers are presented in Table 2. Performance of the classifiers is evaluated by the number of false alarms and undetected faults. False alarms refer to classification of normal inputs as abnormal, and undetected faults represent cases where the classifiers did not identify tool breakage. The SCBC produced perfect detection for all the tests; the Kohonen's method failed to detect tool breakage only in Test #5; and the ART2 produced one false alarm for Test #3, five undetected faults for Test #5, and two false alarms and one undetected fault for Test #6. Referring to the results in Figs. 3-6

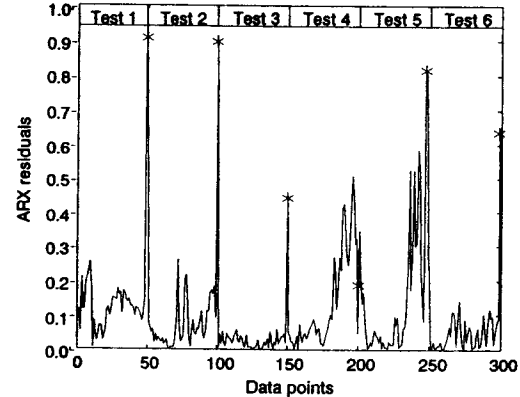


Figure 6: Selected residuals of the ARX model for the six tests. Tool breakages are indicated by the asterisks.

it can be observed that the ART2 had particular difficulty with noisy data (e.g., Test #6). It should be noted that the results for the ART2 represent its best performance, obtained after many trials within a broad range of parameter settings.

The utility of a detection system depends on its ability to adapt to changing process conditions. For the purpose of testing the adaptation ability of the classifiers, the data from the tests were presented to the classifiers in different sequences (see Table 3). The results indicate that the SCBC was completely insensitive to the sequence in which the data was presented to it. The Kohonen's method produced one undetected fault for all the sequences, as expected, due to its batch type of operation which makes it insensitive to data sequence. The ART2 produced a large number of false alarms and undetected faults for Cases #4, #5, and #6. The superior ability of the SCBC to adapt is mainly due to its noise control using *contrast enhancement* and *voting*.

Test Set	Classifier	False Alarms	Undetected Faults
#1	SCBC	0	0
	Kohonen's	0	0
	ART2	0	0
#2	SCBC	0	0
	Kohonen's	0	0
	ART2	0	0
#3	SCBC	0	0
	Kohonen's	0	0
	ART2	1	0
#4	SCBC	0	0
	Kohonen's	0	0
	ART2	0	0
#5	SCBC	0	0
	Kohonen's	0	1
	ART2	0	5
#6	SCBC	0	0
	Kohonen's	0	0
	ART2	2	1

Table 2: Detection results from the SCBC, Kohonen's, and ART2 for individual tests.

6 SUMMARY

A new unsupervised neural network is introduced for tool breakage detection in machining. This classifier performs detection by comparing the measurements only against the normal category, so it does not require any samples of measurements taken at tool breakage to establish an abnormal category. This *Single Category-Based Classifier (SCBC)* also continuously updates the prototype vector representing the normal category to adapt to changing process conditions, and employs both *contrast enhancement* and *voiting* to cope with noise in the measurements. The SCBC was evaluated experimentally in turning where six tool breakage cases were produced. Several sensors were used for instrumentation from which four measurements which were good indicators of tool breakage were obtained. These measurements were then used as inputs to the SCBC and two other unsupervised classifiers. The SCBC was able to detect all the failures without producing any false alarms.

Case #	Sequence	Classifier	False Alarms	Undetected Faults
1	123456	SCBC	0	0
		Kohonen's	0	1
		ART2	1	0
2	124653	SCBC	0	0
		Kohonen's	0	1
		ART2	1	0
3	134265	SCBC	0	0
		Kohonen's	0	1
		ART2	1	0
4	245163	SCBC	0	0
		Kohonen's	0	1
		ART2	5	4
5	354216	SCBC	0	0
		Kohonen's	0	1
		ART2	3	0
6	564321	SCBC	0	0
		Kohonen's	0	1
		ART2	5	3
7	612453	SCBC	0	0
		Kohonen's	0	1
		ART2	6	3
8	654321	SCBC	0	0
		Kohonen's	0	1
		ART2	6	3

Table 3: Detection results from the SCBC, Kohonen's, and ART2 when tests were presented in different sequences to the classifiers.

ACKNOWLEDGEMENTS

The authors would like to express their gratitude to S. R. Hayashi and B. Keramati from GE Corporate Research for their support during the experimental phase of this project. This work was supported in part by the National Science Foundation (Grant No. MSS-9102149).

REFERENCES

- [1] Carpenter, G. A., and Grossberg, S., 1987, "ART2: Self-Organization of Stable Category Recognition Codes for Analog Input Patterns," *Applied Optics*, Vol. 26, pp. 4919-4930.
- [2] Colgan, J. H., Chin, H., Danai, K., and Hayashi, S. R., 1992, "On-line Tool Breakage Detection in Turning: A Multi-Sensor Method," *Sensors and Signal Processing for Manufacturing*, ASME, PED-Vol. 55, pp. 33-43.
- [3] Hayashi, S. R., Thomas C. E., and Wildes, D. G., 1988, "Tool Break Detection By Monitoring Ultrasonic Vibrations," *Annals of the CIRP*, Vol. 37, No. 1, pp. 61-64.
- [4] Hertz, J., Krogh, A., and Palmer, R. G., editors, 1991, *Introduction to the Theory of Neural Computation*, Addison-Wesley, Redwood City, CA.
- [5] Isermann, R., 1984, "Process Fault Detection Based on Modeling and Estimation Methods - A Survey," *Automatica*, Vol. 20, No. 4, pp. 387-404.
- [6] Koenig, W., Kluft, W., and Froehlich, R., 1978, "Automatische Werkzeugbrucherkennung bei der Drehbearbeitung (Automated Detection of Tool-Breakage in Turning)," *Industrie-Anzeiger*, Vol. 100, No. 28, pp. 62-63.
- [7] Kohonen, T., 1989, *Self-Organization and Associative Memory*, 3rd Edition, Springer Verlag, Berlin.
- [8] Lan, M. S., and Dornfeld, D. A., 1984, "In-Process Tool Fracture Detection," *ASME Journal of Engineering Materials and Technology*, Vol. 106, April, pp. 111-118.
- [9] Ljung, L., 1987, *System Identification - Theory for the User*, Prentice-Hall, Englewood Cliffs, NJ.
- [10] Matsushima, K., Bertok, P., and Sata, T., 1982, "In-Process Detection of Tool Breakage by Monitoring the Spindle Current of Machine Tool," *Measurement and Control for Batch Manufacturing*, ASME, pp. 145-154.
- [11] Moriwaki, T., 1980, "Detection for Tool Fracture by Acoustic Emission Measurement," *Annals of the CIRP*, Vol. 29, No. 1, pp. 35-40.
- [12] Tansel, I. N., McLaughlin, C., 1991, "On-Line Monitoring of Tool Breakage with Unsupervised Neural Networks," *Trans. of NAMRC*, SME, pp. 364-370.